Anisotropy of Antiferromagnetic 180° Domains in $LiCoPO_4$ and $LiNiPO_4$

Bas B. Van Aken,[1] J. P. Rivera,[2] H. Schmid,[2] and M. Fiebig[1,*]

[1]*HISKP, Universität Bonn, Nussallee 14-16, 53115 Bonn, Germany*

[2]*Department of Inorganic, Analytical and Applied Chemistry, University of Geneva, 30 quai Ernest-Ansermet, 1211 Geneva 4, Switzerland*

(Received 9 July 2008; published 8 October 2008)

Unexpected three-dimensional distributions of antiferromagnetic 180° domains are observed in $LiCoPO_4$ and $LiNiPO_4$ by optical second harmonic generation. Domains in $LiCoPO_4$ are isotropic in spite of the quasi-two-dimensional magnetic structure whereas domains in $LiNiPO_4$ are distinctly anisotropic, but in contrast to the anisotropy of the magnetic structure. The diversity reveals a potential for fine-tuning magnetic properties determined by the distribution of domains or domain walls and the urgent need for an improved understanding of spatial correlations in antiferromagnets.

DOI: 10.1103/PhysRevLett.101.157202 PACS numbers: 75.60.Ch, 42.65.Ky, 75.30.Gw, 75.50.Ee

In recent years the significance of antiferromagnetism for practical applications has continuously been increasing. Most of the practical interest in antiferromagnetic (AFM) compounds is focused on the exchange-bias effect [1]. In basic research, AFM phase transitions and correlations play an important role in strongly correlated systems [2,3]. Finally, the absence of a macroscopic magnetization makes AFM compounds candidates for extremely rapid spin manipulation since there is no angular momentum to be conserved [4]. The AFM state, just like the ferromagnetic state, is characterized by the presence of domains. In fact, the distribution of AFM domains is essential for exchange bias and certain magnetoresistance phenomena. Profound analysis of the mechanisms determining the topology of AFM domains is therefore highly desirable.

Unfortunately this is hampered by two complications. On the one hand, the magnetic field energy is zero in AFM compounds. Therefore the AFM domain topology is determined by subtle, less well understood criteria like gradient fields in domain walls, magnetostriction, anisotropy, and defects. The most subtle class of AFM domains are the 180° domains: they differ in the respective reversal of all spins only. Unlike in compounds like NiO [5,6] their walls are not subject to strain or other mechanical or electrostatic effects so that the investigation of compounds forming 180° domains directly leads to the inherent magnetic effects determining the AFM domain topology. Their revelation is desirable because in spite of their intrinsic nature the orientation of 180° degree domains determines technologically relevant parameters such as the sign of the exchange-bias effect [7].

On the other hand, experimental techniques for imaging AFM domain structures are rare. The topology of AFM 180° degree domains is particularly difficult to analyze, mostly requiring polarized neutrons for their observation [8]. A very convenient way for imaging long-range ordered structures, and, in particular, AFM 180° domains is optical second harmonic generation (SHG) [9,10]. A light field $\vec{E}$ at frequency ω is incident on a crystal and induces a polarization $\vec{P}$ at frequency 2ω which acts as the source of a frequency-doubled light wave. This is expressed by

$$\vec{P}(2\omega) = \epsilon_0 \hat{\chi}\, \vec{E}(\omega)\vec{E}(\omega) \tag{1}$$

with $\hat{\chi}$ as SHG susceptibility including contributions that couple linearly to the AFM order parameter. Thus, SHG distinguishes between opposite 180° domains through a change of sign of $\vec{P}(2\omega)$ corresponding to a 180° phase difference between the corresponding SHG light waves [11]. However, only a few crystals, all of them uniaxial with light incident along the optical axis, were studied thus far. This limited the investigations to the isotropic case while the influence of magnetic anisotropy on the geometry of bulk AFM 180° domains remained unclear.

Here we report on the observation of AFM 180° bulk domains in the highly anisotropic $LiMPO_4$ system (here M = Co, Ni). SHG coupling linearly to the AFM order parameter was identified in spectroscopy measurements and used for imaging domains whose lateral dimension were found to range between 10 μm and 1 mm. The $LiCoPO_4$ domains were found to be insensitive to the magnetocrystalline anisotropy. In contrast, the $LiNiPO_4$ domains form anisotropic distributions, although in an unexpected way. This diversity, despite the very similar crystallographic and magnetic structure of the $LiMPO_4$ compounds, complicates the understanding of AFM 180° domains but it also points to a great flexibility in tuning the domain structure towards technological requirements.

$LiMPO_4$ has the centrosymmetric olivine crystal structure with $mmm1'$ point symmetry in the paramagnetic state and four formula units per unit cell [12,13]. The optical transmission of the $LiMPO_4$ compounds is determined by d-d transitions from the $^4T_{1g}(F)$ and the $^3A_{2g}(F)$ ground state of the octahedrally coordinated $Co^{2+}(3d^7)$ and $Ni^{2+}(3d^8)$ ions, respectively, which were understood on the basis of ligand-field theory [14,15]. Below T_N = 21.8 K long-range AFM order is present in both compounds which is quasi-two-dimensional with respect to

the yz plane but supported by superexchange along the M-O-M and M-O-P-O-M bonds [16,17]. Originally the same compensated arrangement of up and down spins was derived by neutron diffraction for $LiCoPO_4$ and $LiNiPO_4$, the only difference being the spin direction which is along y for the Co^{2+} and along z for the Ni^{2+} spins, leading to mmm' and $mm'm$, respectively, as magnetic point symmetry [18]. Later, subtle deviations were revealed. In $LiCoPO_4$ the magnetic moments are rotated by 4.6° away from the y axis in the whole temperature range up to T_N [13]. In $LiNiPO_4$ spin rotation occurs only in the range from $T_N - 1$ K to T_N in the form of an incommensurate cycloid [19,20]. In addition, both compounds revealed a very weak spontaneous magnetization along the spin direction [19].

Access to this structure by SHG is governed by the Neumann principle: Any symmetry operation applied to a system leaves its physical properties invariant. This determines the set of nonzero and independent tensor components in Eq. (1) [21]. In turn, experimental determination of these tensor components reveals the crystallographic and magnetic symmetry and structure of a compound. SHG in the electric-dipole approximation of Eq. (1) is only allowed in noncentrosymmetric compounds. In $LiMPO_4$ the AFM spin arrangement breaks the inversion symmetry so that SHG provides a background-free probe of the magnetic (or toroidic [22]) order.

In the experiment sets of three $LiCoPO_4$ and three $LiNiPO_4$ bulk single crystals with lateral dimensions of 2–3 mm and a thickness of 103 μm were used. The three platelets of a set were cut along the (100), (010), and (001) plane, respectively, and had been polished with an aqueous colloidal silica slurry. A transmission setup was employed in which the samples were mounted in a cryostat and excited with 3 ns light pulses of ~1 mJ emitted from an optical parametric oscillator. The polarization of the incident light was set with a half-wave plate. Behind the cryostat, the polarization was analyzed with a filter while the fundamental light was suppressed by high-pass color filters. The SHG light was projected onto a liquid-nitrogen cooled digital camera by a telephoto lens.

Figure 1 shows the SHG spectra of $LiCoPO_4$ and $LiNiPO_4$ taken at 10 K in the range 1.8–3.0 eV. The intensity of the SHG light emitted by the samples results from a convolution of the SHG susceptibility with the linear absorption of the incident fundamental light, the linear absorption of the frequency-doubled light generated in the sample, and phase-matching issues. Therefore, the peak positions of the SHG spectra do not coincide with the energies of d-d transitions in optical transmission data [14,15]. A major advantage of the investigation of magnetic structures by SHG is that for the symmetry analysis only the spectral and polarization dependence of the SHG signal is needed, but not its relation to the explicit optical transitions. Spectroscopy reveals that nonzero contributions to SHG in $LiCoPO_4$ are χ_{zxx}, χ_{xxz}, χ_{zyy}, χ_{yyz}, χ_{zzz}, χ_{yzz}, χ_{yyy}. This points uniquely to the magnetic point symmetry $2'_x$ [21] in agreement with recent neutron diffraction data [13]. Note that if χ_{yzz} and χ_{yyy} whose SHG contributions are 2–4 orders of magnitude weaker than the other contributions, are neglected the point symmetry mmm' is obtained which is the symmetry originally proposed for $LiCoPO_4$. Thus, SHG data, just like neutron diffraction data, reveal a small deviation from the higher symmetry which is caused by the small 4.6° rotation of the Co^{2+} spins away from the y axis. For $LiNiPO_4$ an explicit statement on the absence or presence of such a spin rotation is not documented. According to the SHG data a spin rotation is absent or at least more than 1 order of magnitude smaller than in $LiCoPO_4$. The nonzero tensor components are χ_{yxx}, χ_{xxy}, χ_{yyy}, χ_{yzz} in agreement with $mm'm$ as magnetic point symmetry whereas none of the components specific for the point group $2'_x$ [21] were observed.

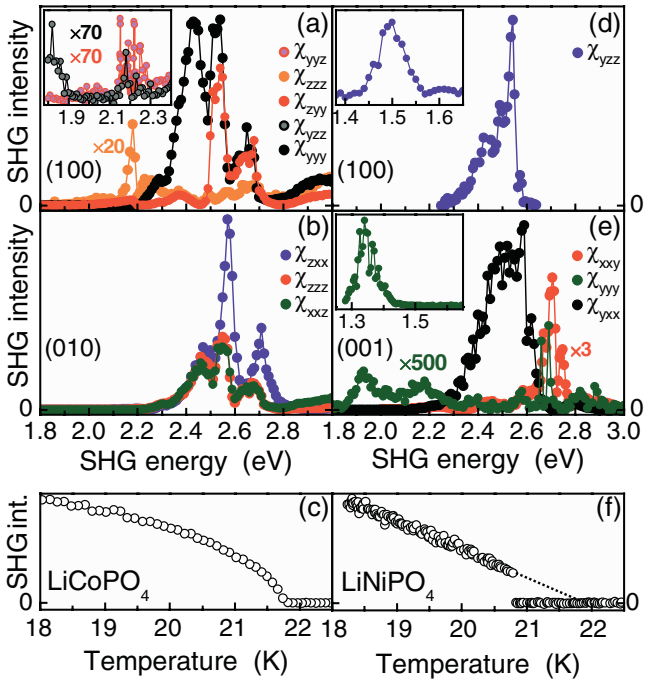

FIG. 1 (color). Spectral and temperature dependence of SHG in $LiCoPO_4$ (a)–(c) and $LiNiPO_4$ (d)–(f). Bias of all insets is zero. The inset in (a) and panel (a) use the same absolute scale; all other intensities are arbitrary scales. Spectra were taken at 10 K. Temperature dependence was measured at 2.50 eV.

The magnetic origin of our SHG signal is confirmed by its temperature dependence. In $LiCoPO_4$ the SHG signal decreases continuously towards zero at T_N. In $LiNiPO_4$ the SHG signal vanishes abruptly at 20.8 K because of the transition to the incommensurate AFM phase but the graphical extrapolation in Fig. 1(f) reveals the literature value $T_N = 21.8$ K.

Any of the tensor components contributing to SHG can be used for probing the AFM domain structure [23]. This leads to Fig. 2 which shows the distribution of the AFM 180° domains on the (100), (010), and (001) faces of the

$LiCoPO_4$ and $LiNiPO_4$ samples at 10 K. The faces of the $LiCoPO_4$ samples reveal dark curved nonintersecting lines on a background of approximately even SHG intensity. The lines correspond to the walls separating opposite 180° domains. Because of the aforementioned 180° phase shift between SHG light from opposite domains destructive interference at the walls leads to a local cancellation [24]. $LiCoPO_4$ reveals an isotropic domain structure with domains of a lateral dimension of 0.1–1 mm. By contrast, the domains observed in $LiNiPO_4$ have a distinctly anisotropic geometry. The (100) and (001) faces reveal domain walls extending across a distance in the order of 1 mm along the x or the z axis, but with tight spacing (~10 μm) along the y axis. On the (010) face a network of curved intersecting lines separating isotropic regions of different brightness with lateral dimensions in the order of 0.1 mm is observed. The $LiNiPO_4$ patterns are caused by platelets of AFM 180° domains parallel to the xz plane and stacked along the y axis. Perpendicular to the (010) face the domains are so thin that light from two or more stacked domains interferes, thus producing differently shaded regions and a pseudointersection of domain walls as quantitatively discussed for Fig. 3.

Figure 2 is remarkable in three ways. First, the degree of difference in the domain topology of $LiCoPO_4$ and $LiNiPO_4$ is striking in view of the aforementioned similarity of the crystallographic and magnetic structure of the two compounds. Second, the isotropic shape of the $LiCoPO_4$ domains is surprising in view of the anisotropic nature of the crystallographic and the quasi-two-dimensional nature of the magnetic $LiMPO_4$ lattice. Third, although the $LiNiPO_4$ domains display a distinct anisotropy it does not correspond to the anisotropy of the compound. The quasi-two-dimensional magnetic order distinguishes the yz plane from the x axis. However, massive formation of domain walls does not occur along the x, but along the y axis whereas the domain distribution is isotropic in the xz plane although the strength of the magnetic coupling in the x and the z direction differs by a factor 20 [16]. It may be expected that the lamellar domain structure in $LiNiPO_4$ is coupled to magnetoelastic deformations. Yet, we detected no elastic domains in linear polarization-optical experiments. We note that the domain structures in Fig. 2 are changed by temperature cycles through T_N but they are not affected by a variation of the cooling rate through or temperature cycles below T_N.

In order not to limit our discussion of bulk domains to their observation at the surface Fig. 3 shows the distribution of SHG intensity on a $LiCoPO_4$ (010) sample at two photon energies. Both images were taken from the same domain structure but while Fig. 3(a) shows domain walls as in Fig. 2, Fig. 3(b) reveals a pattern of laminar fringes of different brightness. In Fig. 3(a) the absorption length at the SHG frequency (2.40 eV) is of the order of 10 μm so that only light from a thin layer contributes to the SHG

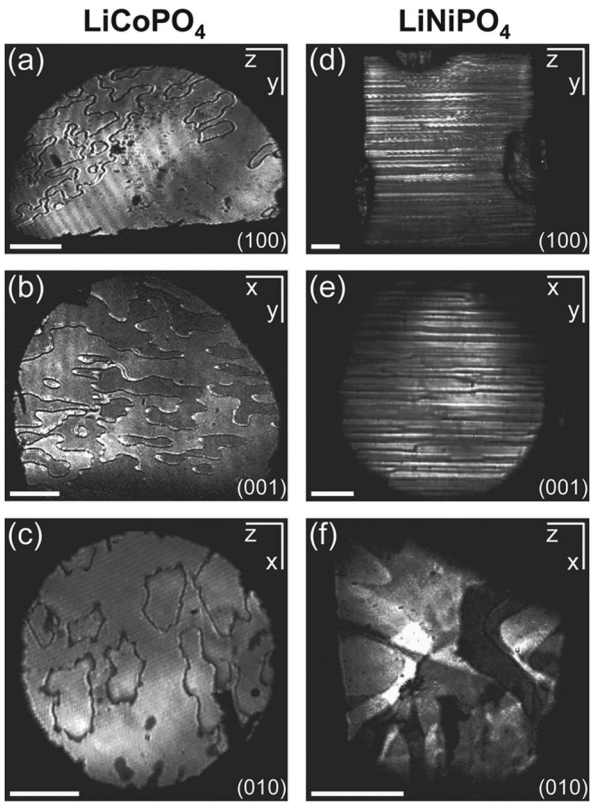

FIG. 2. SHG images of $LiCoPO_4$ and $LiNiPO_4$. Temperature was 10 K. White bars correspond to 0.3 mm.

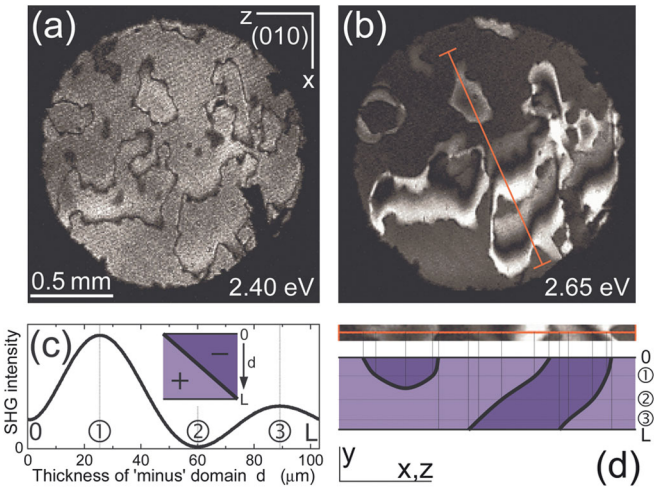

FIG. 3 (color). Three-dimensional domain topology of $LiCoPO_4$ (010). (a) SHG image at 10 K and $2\hbar\omega = 2.40$ eV. (b) SHG image at 10 K and $2\hbar\omega = 2.65$ eV. (c) SHG intensity obtained from Eq. (2) for two domains stacked perpendicular to the surface in dependence of the thickness d of the "−" domain. Values used for the simulation: sample thickness $L = 103$ μm, absorption coefficient (at 2.65 eV) $\alpha = 185$ cm^{-1} (from Ref. [15]), phase mismatch $\Delta k = 1015$ cm^{-1} [from fit of minimum and maximum SHG intensities in (b)]. (d) Domain structure perpendicular to the surface for the section in (b) derived graphically from (b) and (c). Horizontal lines are taken from the maxima and minima in (c). Vertical lines correspond to the position of the maxima and minima in the section.

intensity which therefore displays the AFM domain structure at the surface. In contrast, the absorption length at the SHG frequency (2.65 eV) in Fig. 3(b) is of the order of 100 μm. In this case the amplitude of the SHG intensity for a sample of thickness L is given by [10]

$$A_{\mathrm{SHG}} \propto \int_0^L \mathrm{sgn}(\hat{\chi}(s)) e^{(-\alpha + i\Delta k)s} ds, \qquad (2)$$

where $\Delta k = |2\vec{k}(\omega) - \vec{k}(2\omega)|$ and s denotes the distance from the surface. $\mathrm{sgn}(\hat{\chi})$ yields $+1$ and -1 for opposite 180° domains. As Fig. 3(c) shows a linear increase of the thickness of a "$-$" domain on top of a "$+$" domain leads to a damped sinusoidal oscillation of the SHG intensity. Hence, the interference fringes in Fig. 3(b) are caused by slanted domain walls as sketched in Fig. 3(d). Thus, SHG at photon energies with different absorption length $\alpha(2\omega)$ resolves the full three-dimensional domain structure. Figure 3(b) indicates that the domain structure observed at the surface is representative for the bulk domain structure. Contrary to what might be expected from Ref. [25] no surface-related effects are observed.

In summary, $LiCoPO_4$ and $LiNiPO_4$ revealed a surprising distribution of AFM 180° domains. In spite of their similar crystallographic and magnetic structure the two compounds display drastically different domain patterns. The three-dimensional distribution of the $LiCoPO_4$ domains does not reflect the quasi-two-dimensional magnetic nature of the compound and even in the case of $LiNiPO_4$, where an anisotropic domain structure is found, this anisotropy does not correspond to the magnetic and crystallographic anisotropy of the compound.

This unexpected diversity demonstrates the need for a theoretical model on the formation of AFM domains such as Ref. [25]. For such a model the following points distinguishing $LiNiPO_4$ from the other $LiMPO_4$ compounds might be relevant: (i) The spin-orbit coupling in $LiNiPO_4$ is ≥ 2 times larger than in the other compounds [26]; (ii) $LiNiPO_4$ displays a magnetoelectric effect with abnormal temperature dependence not explainable in single-ion or two-ion theory [27]; (iii) $LiNiPO_4$ possesses half or fully filled t_{2g} and e_g bands.

At the present stage, our results demonstrate that, on the one hand, AFM domains are a rich source for novel physics the understanding of which is not only relevant for a general understanding of strongly correlated compounds with AFM phases but also for controlling applications depending on the interaction between AFM and ferromagnetic [28] or AFM and superconducting [29] phases in multilayer heterostructures. On the other hand the diversity of domain structures found in very similar compounds indicates a large potential for fine-tuning magnetic properties whose manifestation is determined by the distribution of domains and domain walls. These include small-field magnetoresistance [30], exchange-bias effects [7], or magnetoelectric properties [31].

The authors thank the DFG (SFB 608, SPP 1133), the EU (STREP MaCoMuFi–No. 033221), and the Swiss NSF for subsidy and R. Boutellier and S. Gentil for help with growing the crystals.

*fiebig@hiskp.uni-bonn.de

[1] W. H. Meiklejohn and C. P. Bean, Phys. Rev. **105**, 904 (1957).
[2] P. W. Anderson, *The Theory of Superconductivity in the High-T_C Cuprate Superconductors* (Princeton University Press, Princeton, 1997).
[3] *Colossal Magnetoresistive Oxides*, edited by Y. Tokura (Gordon and Breach, London, 2000).
[4] A. V. Kimel, A. Kirilyuk, A. Tsvetkov, R. V. Pisarev, and Th. Rasing, Nature (London) **429**, 850 (2004).
[5] W. L. Roth, J. Appl. Phys. **31**, 2000 (1960).
[6] F. U. Hillebrecht *et al.*, Phys. Rev. Lett. **86**, 3419 (2001).
[7] P. Borisov, A. Hochstrat, X. Chen, W. Kleemann, and C. Binek, Phys. Rev. Lett. **94**, 117203 (2005).
[8] M. Schlenker and J. Baruchel, J. Appl. Phys. **49**, 1996 (1978).
[9] *Nonlinear Optics in Metals*, edited by K. H. Bennemann (Clarendon, Oxford, 1999).
[10] Y. R. Shen, *The Principles of Nonlinear Optics* (Wiley, New York, 2002).
[11] M. Fiebig, V. V. Pavlov, and R. V. Pisarev, J. Opt. Soc. Am. B **22**, 96 (2005).
[12] R. E. Newnham and M. J. Redman, J. Am. Ceram. Soc. **48**, 547 (1965).
[13] D. Vaknin, J. L. Zarestky, L. L. Miller, J. P. Rivera, and H. Schmid, Phys. Rev. B **65**, 224414 (2002).
[14] J. P. Rivera, J. Korean Phys. Soc. **32**, S1839 (1998).
[15] G. R. Rossmann, R. D. Shannon, and R. K. Waring, J. Solid State Chem. **39**, 277 (1981).
[16] D. Vaknin *et al.*, Phys. Rev. B **60**, 1100 (1999).
[17] J. M. Mays, Phys. Rev. **131**, 38 (1963).
[18] R. P. Santoro, D. J. Segal, and R. E. Newnham, J. Phys. Chem. Solids **27**, 1192 (1966).
[19] Yu. N. Kharchenko, N. F. Kharchenko, M. Baran, and R. Szymczak, Low Temp. Phys. **29**, 579 (2003).
[20] D. Vaknin, J. L. Zarestky, J. P. Rivera, and H. Schmid, Phys. Rev. Lett. **92**, 207201 (2004).
[21] R. R. Birss, *Symmetry and Magnetism* (North-Holland, Amsterdam, 1966).
[22] B. B. Van Aken, J. P. Rivera, H. Schmid, and M. Fiebig, Nature (London) **449**, 702 (2007).
[23] Ferrotoroidic domains [22] are neglected because ferrotoroidic SHG is much weaker than AFM SHG.
[24] M. Fiebig, D. Fröhlich, Th. Lottermoser, and M. Maat, Phys. Rev. B **66**, 144102 (2002).
[25] H. Gomonay and V. M. Loktev, J. Phys. Condens. Matter **14**, 3959 (2002).
[26] W. Low, in *Solid State Physics*, edited by F. Seitz and D. Turnbull (Academic, New York, 1960).
[27] M. Mercier, Ph.D. thesis, University of Grenoble 1963.
[28] F. Nolting *et al.*, Nature (London) **405**, 767 (2000).
[29] S. Yunoki *et al.*, Phys. Rev. B **76**, 064532 (2007).
[30] N. D. Mathur *et al.*, Nature (London) **387**, 266 (1997).
[31] M. Fiebig, J. Phys. D **38**, R123 (2005).